

HIGGS BOSON PRODUCTION AND PROPERTIES AT THE TEVATRON

Boris Tuchming
(for the CDF and DØ Collaborations)
*Irfu/SPP, CEA Saclay,
91191 Gif-Sur-Yvette, France*



We present the searches for the Standard Model Higgs boson, using the full Run II dataset of the Fermilab Tevatron $p\bar{p}$ collider, collected with the CDF and DØ detectors. A significant excess of events is observed, consistent with the presence of a Standard Model Higgs boson of mass 125 GeV. We also present tests of different spin/parity hypotheses, performed in the $VH \rightarrow Vb\bar{b}$ channels at DØ, and new searches in invisible modes conducted at CDF.

1 Introduction

Now that the Higgs boson of mass $m_H = 125$ GeV has been discovered in 2012 by the ATLAS and CMS Collaborations at LHC^{1,2}, a new era of measurement has started. The Run II of the Tevatron $p\bar{p}$ collider at $\sqrt{s} = 1.96$ TeV started in 2001 and ended in 2011. Over a decade, the results of the Tevatron collaborations, CDF and DØ, have been a bridge between the search era and the measurement era. They provided the first post-LEP constraints on the Standard Model (SM) Higgs boson mass^{3,4}, as well as the evidence that Higgs bosons couple to b-quarks⁵.

This proceedings summarizes the combined results from the Tevatron collaborations (see Refs.^{6,7,8} and references therein) using the full Run II dataset which corresponds to ~ 10 fb⁻¹ of $p\bar{p}$ collisions per experiment. Recent studies on spin/parity and invisible modes are also presented.

2 Search channels and strategy

Within the SM, the branching ratios and the production cross-sections as a function of the Higgs boson mass are well known. Over the mass range $90 < M_H < 200$ GeV, the dominant production process is the gluon-gluon fusion $gg \rightarrow H$ (950 fb for $M_H = 125$ GeV), followed by the associated production with a weak vector boson $p\bar{p} \rightarrow WH$, $p\bar{p} \rightarrow ZH$ (respectively 130 fb and 79 fb for $M_H = 125$ GeV). The main decay modes are $H \rightarrow b\bar{b}$ (58% for $M_H = 125$ GeV) and $H \rightarrow W^+W^-$ (22% for $M_H = 125$ GeV), so that the most sensitive signatures are: i) one lepton + \cancel{E}_T + two b-jets (mainly $WH \rightarrow \ell\nu b\bar{b}$), ii) no lepton + \cancel{E}_T + two b-jets

(mainly $ZH \rightarrow \nu\bar{\nu}b\bar{b}$), iii) two leptons + two b -jets ($ZH \rightarrow \ell^+\ell^-b\bar{b}$), and iv) two leptons + \cancel{E}_T ($H \rightarrow W^+W^- \rightarrow \ell^+\nu\ell^-\bar{\nu}$). Thus, the Higgs physics at Tevatron mainly relies on b -tagging efficiency, good dijet mass resolution, high- p_T lepton acceptance, good modeling of the \cancel{E}_T , and good modeling of the V +jet background (where $V = W$ or Z). The Tevatron sensitivity to $VH \rightarrow Vb\bar{b}$ is complementary to the LHC main discovery channels ($H \rightarrow \gamma\gamma$, $H \rightarrow ZZ$).

The main sensitivity is given by the four channels presented above, but many other signatures are also considered to bring additional sensitivity and test the agreement with the SM expectations. For examples, Tevatron experiments have also looked for diphoton events ($H \rightarrow \gamma\gamma$), associated production with top-quark pairs ($t\bar{t}H$), lepton + \cancel{E}_T + dijet signatures (from $H \rightarrow WW$), trilepton signatures (*e.g.* from $WH \rightarrow WWW$), same charge dilepton signatures (*e.g.* from $WH \rightarrow WWW$), quadrilepton signatures (*e.g.* from $ZH \rightarrow \ell^+\ell^-WW$), and tau-based signatures (*e.g.* from $WH \rightarrow q\bar{q}\tau^+\tau^-$).

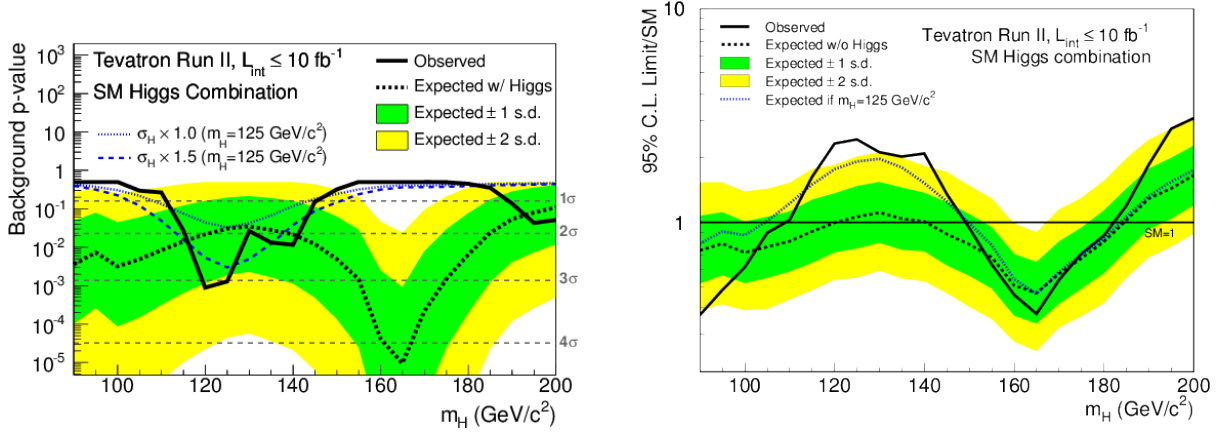
Over the course of Run II, CDF and DØ have followed the same strategy to optimize the analyses and improve their sensitivity:

- Acceptance is maximized by lowering kinematic requirements on leptons, by including different lepton reconstruction categories, by accepting events from all possible triggers, and by optimizing object identification with sophisticated multivariate (MVA) techniques (*e.g.* b -tagging).
- MVA techniques are widely used to maximize use of available information. Using a MVA as a final discriminant typically provides 25% more sensitivity than just using a single kinematic discriminant such as the dijet mass for the $VH \rightarrow Vb\bar{b}$ channels. Dedicated MVA are also trained to split analyses into subchannels enhanced or enriched in specific backgrounds.
- The various channels are split into subchannels according to jet multiplicity, lepton flavor or lepton quality, and b -tagging content. Using subchannels with different signal-over-background ratio (s/b) maximizes discriminating power, allows sensitivity to different signal production modes, and provides more handles and lever-arm to control backgrounds and systematic uncertainties.
- The data are employed as much as possible. Instrumental backgrounds, such as jets or photons faking leptons, charge mismeasurements, and tail of \cancel{E}_T resolution are measured in dedicated control samples. Background enriched samples are also employed to check modeling of specific background processes. Eventually, the same analysis techniques, namely the same kind of MVA, the same subchannels, and the same treatment of systematic uncertainties are employed to measure production rates of known SM candles such as $p\bar{p} \rightarrow W^+W^- \rightarrow \ell^+\nu\ell^-\bar{\nu}$, or $VZ \rightarrow Vb\bar{b}$. For example, the combined CDF+DØ measured cross section $\sigma(WW + WZ) = 3.0 \pm 0.6 \text{ stat} \pm 0.7 \text{ syst pb}^{-1}$ is in agreement with SM prediction of $4.4 \pm 0.3 \text{ pb}^{-1}$.

3 Higgs boson studies

3.1 Search for Standard Model Higgs boson

The results from the different search channels are combined with a log-likelihood ratio (LLR) testing the signal-plus-background over the background-only hypothesis as a function of the Higgs boson mass. The background p-value arising from this test is shown in Fig. 1(a). A significant signal-like excess in the mass range between 115 and 140 GeV is observed. The background p-value of that excess corresponds to 3.0 standard deviation (s.d.) for $M_H = 125$ GeV. That excess arises from both CDF (2.0 s.d.) and DØ (1.7 s.d.) data. The LLR test statistic is also employed to derive limits at 95% C.L. on the Higgs boson production measured in units of the expected SM production. The limits are shown in Fig. 1(b). The combined CDF and DØ results almost reaches the exclusion sensitivity over the full range [90, 185] GeV.



(a) Background p-value as a function of the Higgs boson mass hypothesis.

(b) Limits on the SM Higgs boson production as a function of the Higgs boson mass hypothesis.

Figure 1 – CDF and DØ combined results.

Because of the excess observed in the low mass region, the actual observed exclusion ranges are: [90, 109] GeV and [149, 182] GeV, which is smaller than expected.

3.2 Measurement of production rates

The SM search channels can be separately combined to measure the yield in the different modes: $H \rightarrow b\bar{b}$, $H \rightarrow \tau^+\tau^-$, $H \rightarrow W^+W^-$, and $H \rightarrow \gamma\gamma$. The best fits to the data are summarized in Table 1. Relative to the SM expectation, the overall production rate $R = 1.44^{+0.59}_{-0.56}$ is measured for $M_H = 125$ GeV. The modes with sizable signal-like excesses relative to the background-only hypothesis are $VH \rightarrow Vb\bar{b}$ and $H \rightarrow W^+W^-$, as expected from the SM Higgs boson. The most sensitive channel is $VH \rightarrow Vb\bar{b}$ with a fitted production rate of $R = 1.6 \pm 0.7$. This result is competitive with respect to the measurements of $R(VH \rightarrow Vb\bar{b}) = 0.2 \pm 0.6$ and $R(VH \rightarrow Vb\bar{b}) = 1.0 \pm 0.5$ obtained respectively by the ATLAS⁹ and CMS¹⁰ Collaborations.

3.3 Measurement of couplings to fermions and bosons

Assuming a SM-like Higgs particle of 125 GeV, the SM couplings to fermions and vector bosons are scaled by respectively κ_f , κ_W , and κ_Z , accounting also for the overall scaling of the total width. A fit to the data is performed by scaling properly the contributions from the different production and decay modes, and 2-dimension and 1-dimension posterior density probability are obtained for the coupling scale factors. The 1-dimension constraints on the coupling scale factors

	CDF ⁶	DØ ⁷	CDF+DØ ⁸
$R_{\text{fit}}(H \rightarrow W^+W^-)$	$0.00^{+1.78}_{-0.00}$	$1.90^{+1.63}_{-1.52}$	$0.94^{+0.85}_{-0.83}$
$R_{\text{fit}}(VH \rightarrow Vb\bar{b})$	$1.72^{+0.92}_{-0.87}$	$1.23^{+1.24}_{-1.17}$	$1.59^{+0.69}_{-0.72}$
$R_{\text{fit}}(H \rightarrow \gamma\gamma)$	$7.81^{+4.61}_{-4.42}$	$4.20^{+4.60}_{-4.20}$	$5.97^{+3.39}_{-3.12}$
$R_{\text{fit}}(H \rightarrow \tau^+\tau^-)$	$0.00^{+8.44}_{-0.00}$	$3.96^{+4.11}_{-3.38}$	$1.68^{+2.28}_{-1.68}$
$R_{\text{fit}}(t\bar{t}H \rightarrow t\bar{t}b\bar{b})$	$9.49^{+6.60}_{-6.28}$	–	–
$R_{\text{fit}}(\text{combined SM})$	$1.54^{+0.77}_{-0.73}$	$1.40^{+0.92}_{-0.88}$	$1.44^{+0.59}_{-0.56}$

Table 1: Best fit to the data of the Higgs boson production (in unit of the SM Higgs boson production), assuming $M_H = 125$ GeV, for the different channels and their combination.

are: i) assuming $\kappa_W = \kappa_f = 1$, the best-fit value is $\kappa_Z = \pm 1.05_{-0.55}^{+0.45}$; ii) assuming $\kappa_Z = \kappa_f = 1$, the best-fit 68% confidence intervals are defined by $\kappa_W = -1.27_{-0.29}^{+0.46}$ and $1.04 < \kappa_W < 1.51$; iii) assuming $\kappa_W = \kappa_Z = 1$, the best-fit value is $\kappa_f = -2.64_{-1.30}^{+1.59}$; iv) and by letting κ_f floating with a flat prior, the custodial symmetry is tested and the best fit value for the ratio $\lambda_{WZ} = \frac{\kappa_W}{\kappa_Z}$ reads $\lambda_{WZ} = 1.24_{-0.42}^{+2.34}$. All these results are in agreement with the SM expectations within their uncertainties.

3.4 Spin and parity tests

The tests are based on the property that spin and parity of a particle affects the shape of the excitation curve near the production threshold. Thus, the spectra of the effective center-of mass energy, $\sqrt{\hat{s}}$, of $VH \rightarrow Vb\bar{b}$ events are expected to be quite different under different spin and parity hypotheses (0^- , 0^+ , or 2^+) for H ¹¹. This property is exploited by DØ to re-analyze the data samples from the $VH \rightarrow Vb\bar{b}$ SM Higgs channels¹². DØ uses as discriminant observable the overall mass (or transverse mass for final states with neutrinos) of the candidate events. The signal sensitivity is enhanced by splitting the samples into low and high purity regions, according to the dijet invariant mass (ZH channels) or the SM MVA discriminant output (WH channel). The results are obtained assuming the production times branching fraction ($\sigma \times Br$) of $1.23 \times \text{SM}$ (DØ best fit value for $H \rightarrow b\bar{b}$): i) a 0^+ hypothesis is favored over a 0^- and 2^+ signal at the 99.9% and 99.5%, respectively; ii) a mixture of 0^- and 0^+ signals is excluded at 95% C.L. for fractions of 0^- signal higher than 0.67; iii) a mixture of 2^+ and 0^+ signals is excluded at 95% C.L. for fractions of 2^+ signal higher than 0.57.

3.5 Search for invisible decays

CDF exploits the $Z \rightarrow \ell^+ \ell^- + \text{large } \cancel{E}_T$ signature to search for ZH where H decays to undetected products¹³. The absence of excess in the data allows to set a limit of $\sigma \times Br > 90$ fb for invisible modes for $m_H = 125$ GeV. A 100% branching fraction to invisible particles is excluded if $M_H < 120$ GeV.

4 Conclusion

The final combined results of CDF and DØ exhibits a 3.0 s.d. evidence for the production of the SM Higgs boson. Within their respective uncertainties, the measurements of production rates and couplings show good agreement with the SM expectations. Recent analyses of spin and parity properties and recent searches for invisible decays also exhibit consistency with the SM.

References

1. G. Aad *et al.* [ATLAS Collaboration], Phys. Lett. B **716**, 1 (2012).
2. S. Chatrchyan *et al.* [CMS Collaboration], Phys. Lett. B **716**, 30 (2012).
3. The CDF and DØ Collaborations, arXiv:0808.0534 (2008).
4. T. Aaltonen *et al.* [CDF and DØ Collaborations], Phys. Rev. Lett. **104**, 061802 (2010).
5. T. Aaltonen *et al.* [CDF and DØ Collaborations], Phys. Rev. Lett. **109**, 071804 (2012).
6. T. Aaltonen *et al.* [CDF Collaboration], Phys. Rev. D **88**, 052013 (2013).
7. V. M. Abazov *et al.* [DØ Collaboration], Phys. Rev. D **88**, 052011 (2013).
8. T. Aaltonen *et al.* [CDF and DØ Collaborations], Phys. Rev. D **88**, 052014 (2013).
9. ATLAS Collaboration, ATLAS-CONF-2013-079.
10. S. Chatrchyan *et al.* [CMS Collaboration], Phys. Rev. D **89**, 012003 (2014).
11. J. Ellis, D. S. Hwang, V. Sanz and T. You, JHEP **1211**, 134 (2012).
12. The DØ Collaboration, DØ Note **6387-CONF** (2013), DØ Note **6406-CONF** (2013).
13. The CDF Collaboration, CDF Note **11068** (2014).